

CNRS
Centre National de la Recherche Scientifique

INFN
Istituto Nazionale di Fisica Nucleare



Advanced Virgo single cavity alignment

VIR-109B-08

M. Mantovani

Issue: 1

Date: July 29, 2009

VIRGO * A joint CNRS-INFN Project
Via E. Amaldi, I-56021 S. Stefano a Macerata - Cascina (Pisa)
Secretariat: Telephone (39) 050 752 521 * FAX (39) 050 752 550 * Email W3@virgo.infn.it

Contents

1	Introduction	2
2	Radiation pressure effects - Sidle-Sigg computation	3
2.0.1	Comparison between the computed and simulated eigen-frequencies	4
3	Error signals and optical matrix	6
3.1	Controllability as a function of the input power	6
4	Conclusions	8
A	Finesse <i>vs</i> Optickle - low power regime	9

cavity length L	3000 m	Arm cavity finesse	900
IMX R_C	1416 m	EMX R_C	1646 m
Beam size on IMX	56 mm	Beam size on EMX	65 mm
waist size w_0	8.5 mm	round-trip losses	75 ppm
transmission IMX T	0.7%	transmission EMX T	5 ppm
IMX and EMX diameter	35 cm	IMX and EMX thickness	20 cm
Mirror density	$2.201 \cdot 10^3$ [kg/m ³]	pitch resonant frequency	1.2 Hz

Table 1: Optical and mechanical parameters for the Advanced Virgo X-arm cavity.

1 Introduction

The main differences between the *Advanced Virgo* configuration for the single cavity system with respect to the Virgo configuration is the larger circulating power, due to higher finesse and higher input power, which produces relevant radiation pressure effects; and the spherical-spherical geometry, with respect to the Virgo plano-concave geometry, to improve the thermal noise.

In order to develop the pre-alignment control scheme for the Advanced Virgo scheme, which means the single cavity alignment, the X-cavity has been modelled with a frequency simulation tool, *Optickle*[1]. It includes the higher order mode computation, only the TEM₀₁ mode, and the radiation pressure considering a simple pendulum suspension. The optical parameters used for the simulations are based on the *Advanced Virgo Baseline Design*[2] as listed in Table 1.

In this note the alignment scheme for the single cavity will be studied and it will be based on a Ward-like technique.

2 Radiation pressure effects - Sidle-Sigg computation

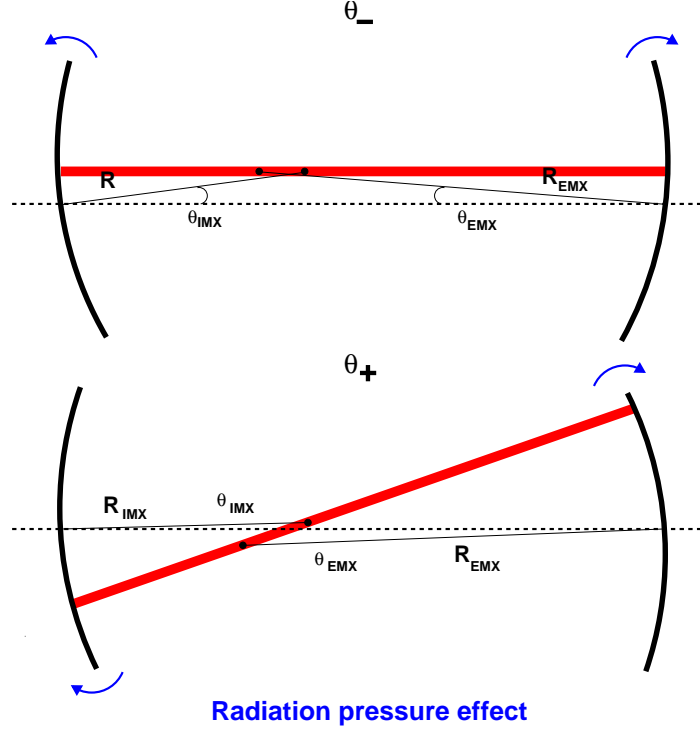


Figure 1: Effect of the radiation pressure in a Fabry-Perot cavity. The two mirror modes become connected by the optical spring and the F-P misalignment can be described in the new base which depends on the optical parameters, (+) *plus* and (-) *minus* showed graphically in the picture.

In an high power Fabry-Perot cavity the radiation pressure connects the two mirrors by an optical spring which modifies the mechanical transfer functions of the two suspension. It can be evaluated analytically by computing the system energy equations, based on the Sidles-Sigg small angle propagation[3], and numerically with Optickle. The kinetic and potential energy can be computed for the whole system as:

$$K_{i,j} = \begin{pmatrix} I_1 & 0 \\ 0 & I_2 \end{pmatrix}$$

$$V_{i,j} = \begin{pmatrix} \mu_1 - \frac{2GP_{in}L}{c} \frac{g_2}{1-g_1g_2} & -\frac{2GP_{in}L}{c} \frac{1}{1-g_1g_2} \\ -\frac{2GP_{in}L}{c} \frac{1}{1-g_1g_2} & \mu_2 - \frac{2GP_{in}L}{c} \frac{g_1}{1-g_1g_2} \end{pmatrix}$$

where I_i is the momentum of inertia of the i-d.o.f.; $\mu_i/I_i = \omega_i^2$ is the torsion pendulum natural frequency; P_{in} is the input power and G is the cavity optical gain, thus $G \cdot P_{in}$ is the stored power inside the cavity; g_i is the cavity parameter, c is the light speed and L is the cavity length. Thus the eigenfrequencies can be computed as $\det(V - \lambda K) = 0$:

$$\omega_+ = \sqrt{\omega_0^2 + \frac{GP_{in}L}{Ic} \frac{-(g_1+g_2)+\sqrt{4+(g_1-g_2)^2}}{(1-g_1g_2)}} \quad (1)$$

$$\omega_- = \sqrt{\omega_0^2 + \frac{GP_{in}L}{Ic} \frac{-(g_1+g_2)-\sqrt{4+(g_1-g_2)^2}}{(1-g_1g_2)}}$$

In the (+)-mode the eigenfrequency increases and the radiation pressure restore the alignment, while in the (-)-mode the eigen-frequency is lowered and the misalignment is worsened. The new base can be written, in

the IMX/EMX base, considering the direction of rotation referred to the front side of the optical component defined by the high-reflective coating, as:

$$\theta_+ = \left(\begin{array}{c} \frac{2}{1-g_1 g_2} \\ \frac{g_1 - g_2 - \sqrt{4 + (g_1 - g_2)^2}}{1 - \frac{1}{2} g_1 g_2} \end{array} \right)$$

$$\theta_- = \left(\begin{array}{c} \frac{2}{1-g_1 g_2} \\ \frac{g_1 - g_2 + \sqrt{4 + (g_1 - g_2)^2}}{1 - g_1 g_2} \end{array} \right)$$

For the Advanced Virgo arm cavity is:

$$\theta_+ = (0.6533, -0.7571) \tag{2}$$

$$\theta_- = (0.7571, 0.6533) \tag{3}$$

$$\tag{4}$$

2.0.1 Comparison between the computed and simulated eigen-frequencies

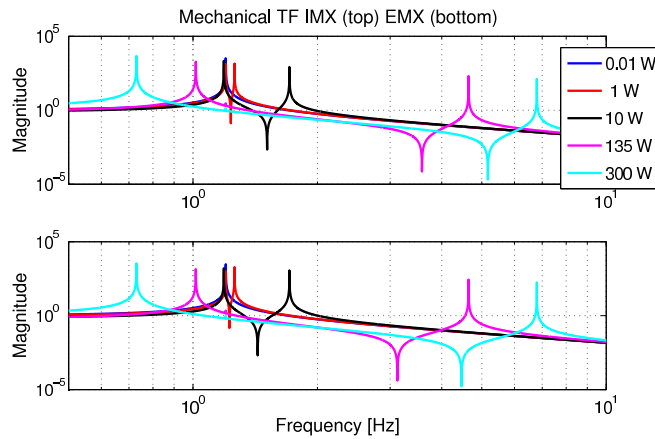


Figure 2: Effect of the radiation pressure on the two mirror mechanical transfer function. The single pendulum transfer function, blue curve for the low power regime, becomes a more complex TF with two resonances, the higher and the lower resonances correspond to the eigen-frequencies.

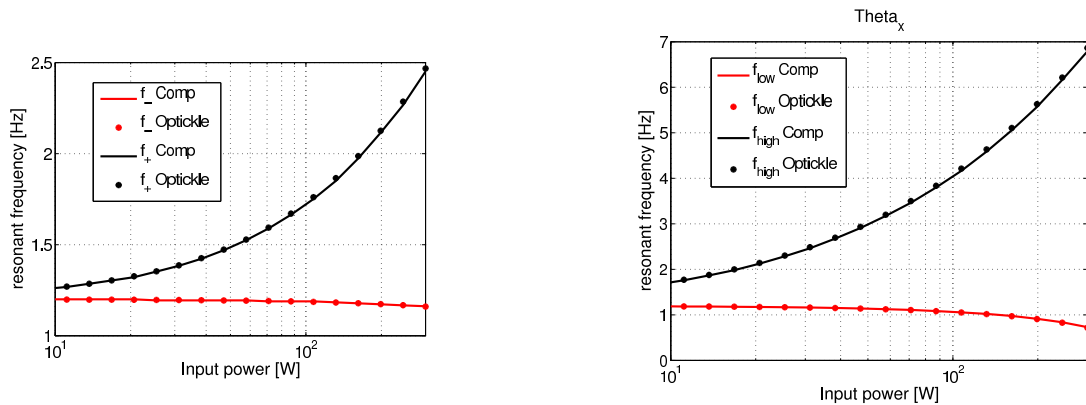


Figure 3: Eigen-frequency comparison, between the computed and the simulated data, as a function of the input power in the single cavity configuration on the left and in the recycled configuration on the right (the PRC optical gain has been taken into account). The plots show a very good agreement between the computed and simulated data, and plot is it clear that the instability, which means negative frequency, can not be reached even with the maximum design power (180 W).

The effect of the radiation pressure on the mechanical transfer function of the mirror suspension is due to the connection of the two single pendulum trough an optical spring. The single pendulum suspension transfer function, blue curve in Figure 2, will become more complex as soon as the radiation pressure effects appear. The mechanical transfer function in the high power regime, for example the cyan curve in Figure 2, shows two resonant frequencies in correspondence of the above computed eigen-frequencies.

In order to validate the modelling of the cavity with Optickle, the eigen-frequencies behaviour as a function of the input power has been studied comparing the analytic and the simulated data, see Figures 3. The eigen-frequency for the (+)-mode increases as the square root of the input power reaching in the not-recycled configuration approximately 2 Hz at full input power and 5.5 Hz in the recycled configuration. This high eigen-frequency results to be very challenging for the control filter design, since they have to be very performing at 10 Hz to do not reintroduce alignment control noise. For the lower eigen-frequency, the (-)-mode, the change in frequency with respect to the low power regime is more moderate and it does not reach the instability, thus negative frequencies, even in the recycling configuration. From now on the mirror base which will be used is the (+) and (-) base, and there will not be any referring to the single mirror modes.

3 Error signals and optical matrix

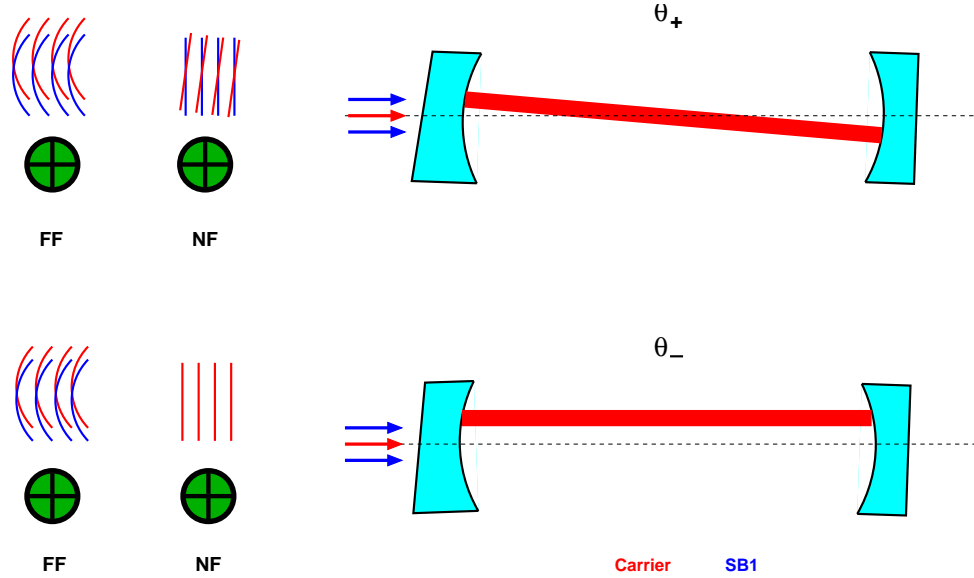


Figure 4: Graphical view of the wave front behaviour in reflection of the cavity for the θ_+ and θ_- modes. The θ_+ mode is well visible in the near-field and far-field quadrant while the θ_- mode is visible essentially only in the far-field quadrant.

The control scheme for the pre-alignment phase, as it was said in the introduction, is based on a Ward-like technique. The Ward technique[4] is a modulation-demodulation method for alignment control based on differential wave front sensing. It requires a modulation frequency which is mostly reflected by the cavity and the error signals will be detected in reflection to the cavity as the beat between the sideband, which is not affected by the cavity mirror misalignments, and the carrier which is resonating in the cavity.

The modulation frequency used to control the cavity alignment is the SB1, 9368110.74 Hz, phase-modulated sideband, proposed for the locking scheme design.

The Figure 4 shows a graphical behaviour of wave front in the near-field and far-field, where the quadrant diodes will be placed, in reflection to the cavity for the (+) and (-) mode misalignment. The (+) mode is detected in both near and far fields while the (-) mode, which is dominated by the translation of the beam with respect to the cavity axis, is essentially detected only in far-field, this should give an almost triangular sensing matrix which ensure the controllability of the system.

In the high power regime the situation is a little bit different since the radiation pressure will increase the (-)-mode misalignment while it will restore the (+)-mode alignment. It is then necessary to study the behaviour of the sensing matrix in case of high circulating power.

3.1 Controllability as a function of the input power

diode	PLUS	MINUS
(P=1 W) POX FF	1	1.1
(P=1 W) POX NF	8	-0.2
(P=135 W) POX FF	59	1.6e+02
(P=135 W) POX NF	4.5e+02	-27

Table 2: Sensing matrix example for 1 and 135 W of input power.

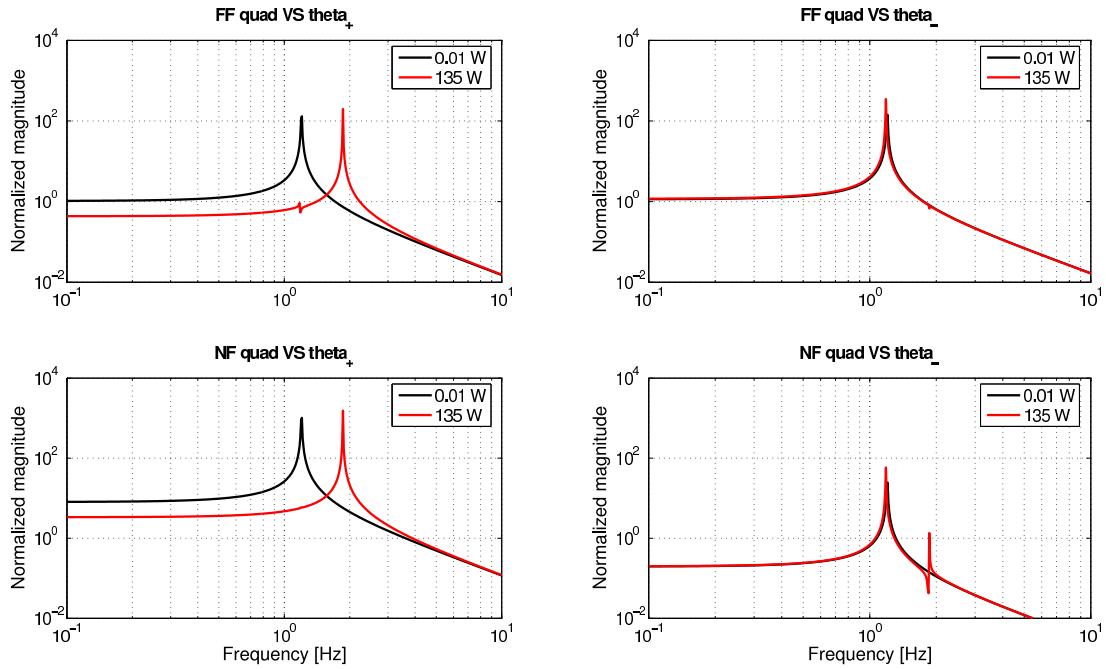


Figure 5: Transfer function between the correction injection point, at the level of the marionette, and the detectors, in near field and far field respectively. The left plots show the behaviour of the (+)-mode for low and high power regime, in the high power regime the (+)-mode is restored thus the error signal is lowered below the resonance.

The sensing matrix has been simulated by placing two quadrant diodes, in near and far field respectively, at the POX detection port, which is the pick-off beam of the IMX mirror, for two input powers: 1 and 135 W ¹. The two d.o.f. becomes more and more decouple increasing the power, since the (+)-mode, which is dominant on all the signals at low power, becomes weaker improving the diagonality of the system.

This behaviour is shown by the sensing matrix in Table: 2 and also by the normalized, on the power, transfer functions between the quadrant diode signal and the point in which the angular correction is applied, at the marionette level, see Figure 5.

The low frequency TF for the (+)-mode is reduced due to the radiation pressure which restores the alignment.

¹The demodulation phase for the quadrant signals has been optimized in order to have the best possible decoupling only at low frequency; while the Gouy phase has been not tuned since experimentally it is quite difficult, thus the diodes are placed in near and far field (0 and 90 deg of Gouy phase).

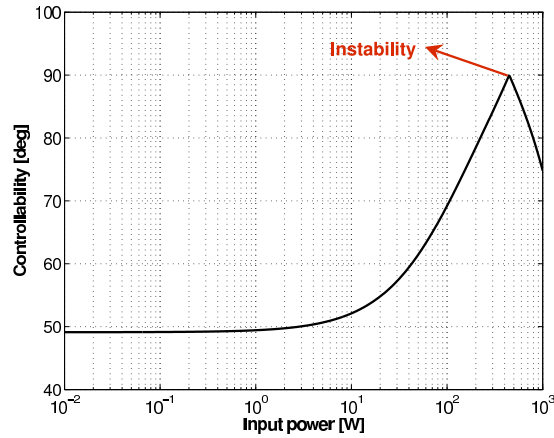


Figure 6: Controllability of the single arm cavity system as a function of the input power. The system becomes more and more decoupled as the input power raises up to the instability point, ~ 450 W.

It can be also evaluated the controllability of the system ²[5]. From Figure 6 the separation angle between the (+) and (-) d.o.f. increases up to 90 deg at the instability point, ~ 450 W, which is well above the normal operation range.

4 Conclusions

The pre-alignment control scheme for the Advanced Virgo configuration will be based on a Ward-like technique using the POX port, pick-off beam at the AR coating of the IMX. The main difference between the Advanced Virgo and the Virgo configuration is the presence of strong radiation pressure effects and the spherical-spherical cavity.

The radiation pressure effects have been studied and it has been concluded that the cavity will be stable also at the maximum stored power of ~ 800 kW, but the (+)-mode eigen-frequency raises up to ~ 6 Hz which will be challenging for the control filter design at 10 Hz.

Moreover the sensing matrix results to be controllable for all the input powers.

² A quality criterion for a designed control system has been developed, which is based on the capability of the sensing scheme to sense the angular position of the d.o.f. to be controlled. The optical configuration is simulated by using the frequency domain simulation software Finesse[6], whose results are processed by Matlab scripts. 0 deg means not controllable while 90 deg means a perfectly controllable system.

A Finesse vs Optickle - low power regime

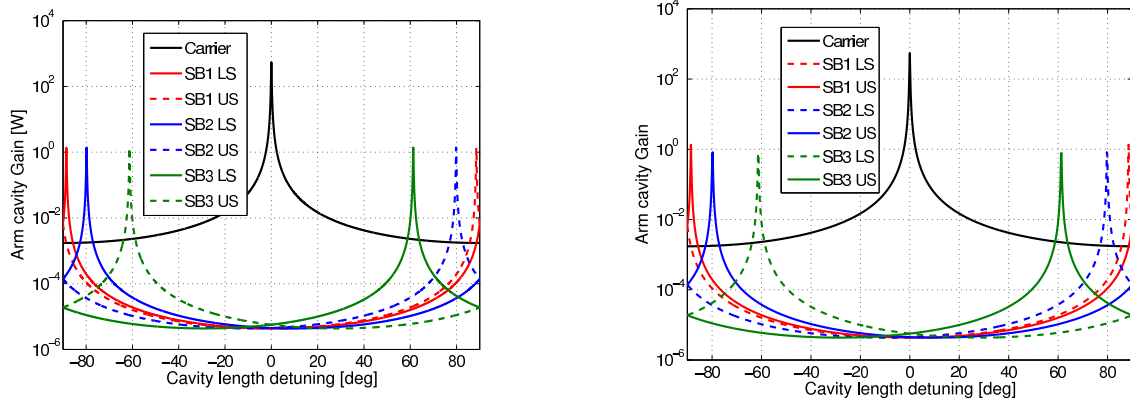


Figure 7: Resonance condition in the arm cavity considering the modulation frequency chosen for the longitudinal control (SB1 9368110.74 Hz phase modulation, SB2= 65576775.21 Hz amplitude modulation, SB3 8327209.55 Hz amplitude modulation) simulated with *optickle* and *finesse* on the left and on the right respectively. The two simulations are well in agreement.

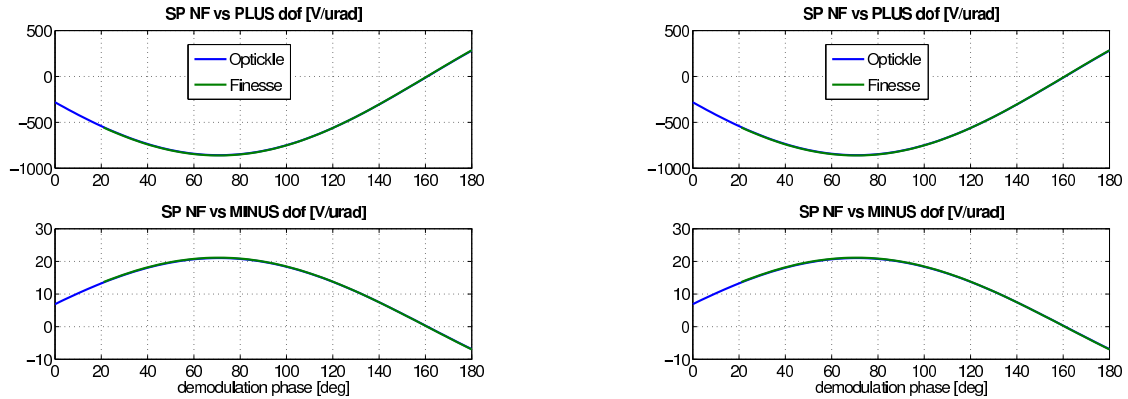


Figure 8: Signals in reflection to the cavity, SP port, simulated with *finesse* and *optickle*. The signals are in agreement within 6-7% in amplitude.

In order to have a further cross-check of the simulation tool *optickle* and of the cavity modelling a comparison between the results obtained with *finesse* and with *optickle* in the low power regime. The resonant condition of the sidebands shown in Figure 7 are coherent and the error signal amplitude as a function of the demodulation phase of the diodes. The amplitude of the signals is the same within 6-7%.

References

- [1] Optickle home-page http://ilog.ligo-wa.caltech.edu:7285/advligo/ISCM_modelingsoftware 2
- [2] Advanced Virgo Baseline Design, VIR-027A-09 (Issue 1), The Virgo Collaboration, May 16, 2009. 2
- [3] D. Sigg *et al.*, *Phys. Lett. A* **354** 3 (2006) 167-172 . 3
- [4] E. Morrison, *Appl. Opt.* **33** (1994), 5041. 6

- [5] M. Mantovani, A. Freise, "Evaluation of Alignment Sensing Matrices using Row Vector Orientation", proceedings of the 7th Amaldi Conference, Sidney 2007. Journal of Physics: Conference Series 122 (2008) 012026. 8
- [6] A. Freise, G. Heinzl, H. Luck, R. Schilling, B. Willke and K. Danzmann, "Frequency domain interferometer simulation with higher-order spatial modes", Class. Quant. Grav. 21 (2004) S1067. 8